Mon. Not. R. Astron. Soc. **000**, 1–?? (2009) Printed 28 January 2009 (MN LATEX style file v2.2)

On the formation of massive galaxies: A simultaneous study of number density, size and intrinsic colour evolution in GOODS

Ignacio Ferreras[1⋆], Thorsten Lisker[2], Anna Pasquali[3], Sadegh Khochfar[4], Sugata Kaviraj[1,5]
[1] *Mullard Space Science Laboratory, Unversity College London, Holmbury St Mary, Dorking, Surrey RH5 6NT*
[2] *Astronomisches Rechen-Institut, Zentrum für Astronomie, Universität Heidelberg, Mönchhofstr. 12-14, D-69120 Heidelberg, Germany*
[3] *Max-Planck-Institut für Astronomie, Koenigstuhl 17, D-69117 Heidelberg, Germany*
[4] *Max-Planck-Institut für Extraterrestrische Physik, Giessenbachstrasse, D-85748 Garching, Germany*
[5] *Astrophysics subdepartment, The Denys Wilkinson Building, Keble Road, Oxford OX1 3RH*

January 20, 2009: To be published in MNRAS

ABSTRACT
The evolution of number density, size and intrinsic colour is determined for a volume-limited sample of visually classified early-type galaxies selected from the HST/ACS images of the GOODS North and South fields (version 2). The sample comprises 457 galaxies over 320 arcmin^2 with stellar masses above $3 \cdot 10^{10}$M$_\odot$in the redshift range 0.4<z<1.2. Our data allow a simultaneous study of number density, intrinsic colour distribution and size. We find that the most massive systems ($\gtrsim 3 \cdot 10^{11} M_\odot$) do not show any appreciable change in comoving number density or size in our data. Furthermore, when including the results from 2dFGRS, we find that the number density of massive early-type galaxies is consistent with no evolution between z=1.2 and 0, i.e. over an epoch spanning more than half of the current age of the Universe. Massive galaxies show very homogeneous *intrinsic* colour distributions, featuring red cores with small scatter. The distribution of half-light radii – when compared to z$\sim$0 and z>1 samples – is compatible with the predictions of semi-analytic models relating size evolution to the amount of dissipation during major mergers. However, in a more speculative fashion, the observations can also be interpreted as weak or even no evolution in comoving number density *and size* between 0.4<z<1.2, thus pushing major mergers of the most massive galaxies towards lower redshifts.

Key words: galaxies: evolution — galaxies: formation — galaxies: luminosity function, mass function — galaxies: high redshift

1 INTRODUCTION

During the past decades the field of extragalactic astrophysics has undergone an impressive development, from simple models that were compared with small, relatively nearby samples to current surveys extending over millions of Mpc^3 at redshifts beyond z$\sim$1 along with numerical models that can probe cosmological volumes with the aid of large supercomputers. However, in the same period of time, our knowledge of the 'baryon physics' relating the dark and luminous matter components has progressed much slower, mainly due to the highly non-linear processes that complicate any ab initio approach to this complex problem.

The evolution of the most massive galaxies constitutes one of the best constraints one can impose on the modelling of galaxy formation. Within the current paradigm of galaxy growth in a ΛCDM cosmology, massive galaxies evolve from subsequent mergers of smaller structures. The most massive galaxies are early-type in morphology and are dominated by old stellar populations, with a tight mass-metallicity relation and abundance ratios suggesting a quick build-up of the stellar component (see e.g. Renzini 2006). On the other hand, semi-analytic models of galaxy formation predict a more extended assembly history (if not star formation) from major mergers. By carefully adjusting these models, it has been possible to generate realizations that are compatible with the observed stellar populations in these galaxies (e.g. Kaviraj et al. 2006; De Lucia et al. 2006; Bower et al. 2006)

In this paper we study the redshift evolution of a sample of the most massive early-type galaxies from the catalogue of Ferreras et al. (2009), which were visually selected from the *HST*/ACS images of the GOODS North (HDFN) and South (CDFS) fields (Giavalisco et al. 2004). Our data set complements recent work exploring the issue of size and stellar mass evolution (e.g. Bundy et al. 2005; McIntosh et al. 2005; Franceschini et al. 2006; Fontana et al. 2006; Borch et al. 2006; Brown et al. 2007; Trujillo et al. 2007; van Dokkum et al. 2008). The coverage (320 arcmin^2), depth (1σ surface brightness limit per pixel of 24.7 AB mag/arcsec^2 in the i band) and high-resolution (FWHM~ 0.12 arcsec) of these images allow us to perform a con-

⋆ E-mail: ferreras@star.ucl.ac.uk

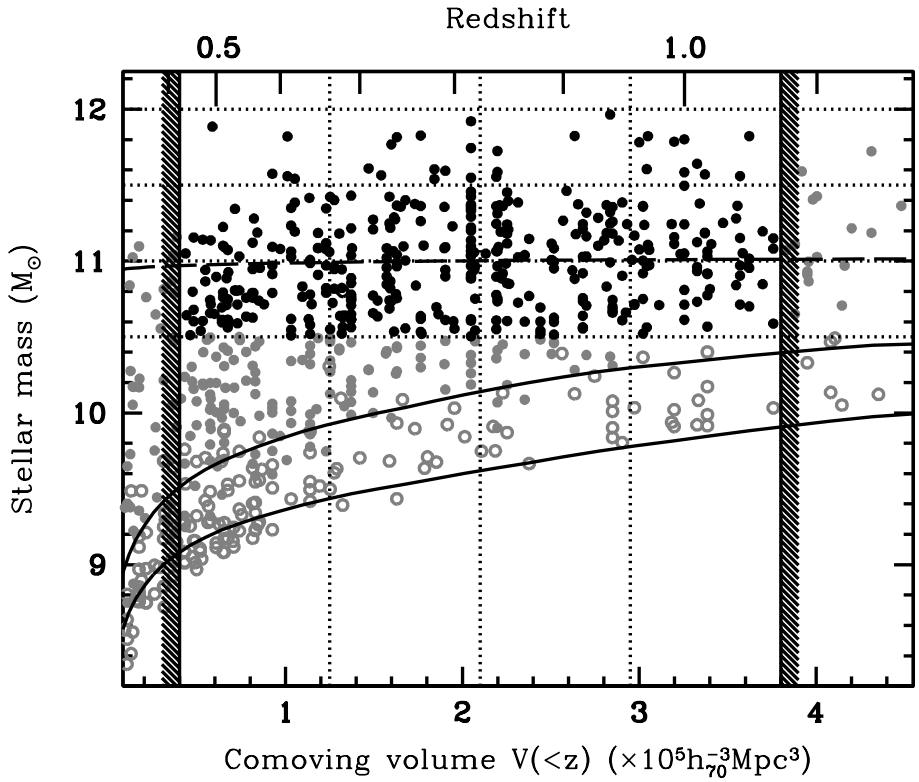

Figure 1. Sample of massive spheroidal galaxies extracted from the v2.0 ACS/HST images of the GOODS North and South fields (Ferreras et al. in preparation). We show in black the volume-limited sub-sample used in this paper. We further subdivide this sample into three mass bins, between $3 \cdot 10^{10}\mathrm{M}_\odot$and $10^{12}\mathrm{M}_\odot$(stellar mass), and in four redshift bins (top axis) centered around z=0.5, 0.7, 0.9 and 1.0 (corresponding to look-back times of 5, 6.3, 7.3, and 7.7 Gyr before present, respectively). The dashed line tracks the characteristic stellar mass (M_*) from GOODS-MUSIC (Fontana et al. 2006). The curved solid lines are the limiting ($i_{AB} = 24$) masses for two exponentally decaying star formation histories with solar metallicity, started at redshift z_F=3 and with formation timescales $\tau = 1$ (top) and 8 Gyr (models of Bruzual & Charlot 2003). Our sample is classified according to a best fit template which roughly separates into 'red' and 'blue' galaxies, represented in this figure as filled and hollow circles, respectively.

sistent analysis of the redshift evolution of the comoving number density, size and intrinsic colour of these galaxies.

2 THE SAMPLE

The *HST*/ACS images of the GOODS North and South fields (v2.0) were used to perform a visual classification of spheroidal galaxies. This is a continuation of Ferreras et al. (2005) – that was restricted to the CDFS field. However, notice that our sample does *not* apply the selection based on the Kormendy relation, i.e. the only constraint in this sample is visual classification. The analysis of the complete sample is presented in Ferreras et al. (2009). Over the 320 arcmin^2 field of view of the North and South GOODS/ACS fields, the total sample comprises 910 galaxies down to $i_{\rm AB} = 24$ mag (of which 533/377 are in HDFN/CDFS). The available photometric data – both space and ground-based – were combined with spectroscopic or photometric redshifts in order to determine the stellar mass content. Spectroscopic redshifts are available for 66% of the galaxies used in this paper. The photometric redshifts have an estimated accuracy of $\Delta(z)/(1+z) \sim 0.002 \pm 0.09$ (Ferreras et al. 2009). Stellar masses are obtained by convolving the synthetic populations of Bruzual & Charlot (2003) with a grid of exponentially decaying star formation histories (see appendix B of Ferreras et al. 2009, for details). A Chabrier (2003) Initial Mass Function is assumed. Even though the intrinsic properties of a stellar population (i.e. its age and metallicity distribution) cannot be accurately constrained with broadband photometry, the stellar mass content can be reliably determined to within $0.2-0.3$ dex provided the adopted IMF gives an accurate representation of the true initial mass function (see e.g. Ferreras et al. 2008).

The sizes are computed using a non-parametric approach that measures the total flux within an ellipse with semimajor axis $a_{\rm TOT} < 1.5 a_{\rm Petro}$. The eccentricity of the ellipse is computed from the second order moments of the surface brightness distribution. The half-light radius is defined as $\mathrm{R}_{50} \equiv \sqrt{a_{50} \times b_{50}}$, where a_{50} and b_{50} are respectively the semimajor and semiminor axes of the ellipse that engulfs 50% of the total flux. Those values need to be corrected for the loss of flux caused by the use of an aperture (see e.g. Graham et al. 2005). We used a synthetic catalogue of galaxies with Sersic profiles and the same noise and sampling properties as the original GOODS/ACS images to build fitting functions for the corrections in flux and size. The corrections depend mostly on R_{50} and, to second order, on the Sersic index. Most of this correction is related to the ratio between the size of the object and the size of the Point Spread Function of the observations. The dependence with Sersic index (or in general surface brightness slope) is milder and

for this correction the concentration (as defined in Bershady et al. 2000) was used as a proxy.

We compared our photometry with the GOODS-MUSIC data (Grazian et al. 2006) in the CDFS. Our sample has 351 galaxies in common with that catalogue, and the difference between our total+corrected i-band magnitudes and the total magnitudes from GOODS-MUSIC is $\Delta i \equiv i_{\rm ours} - i_{\rm MUSIC} = -0.17 \pm 0.16$ mag. This discrepancy is mostly due to our corrections of the total flux. A bootstrap method using synthetic images show that our corrections are accurate with respect to the true total flux to within 0.05 mag, and to within 9% in half-light radius (see appendix A of Ferreras et al. 2009). Our estimates of size were also compared with the GALFIT-based parametric approach of Häussler et al. (2007) on the GEMS survey. Out of 133 galaxies in common, the median of the difference defined as $(\mathrm{R}_{50}^{\rm ours}-\mathrm{R}_{50}^{\rm GEMS})/\mathrm{R}_{50}^{\rm ours}$ is -0.01 ± 0.16 (the error bar is defined as the semi-interquartile range).

We focus here on a volume-limited sample comprising early-type galaxies with stellar mass $M_s \gtrsim 3 \times 10^{10}\mathrm{M}_{\odot}$. This sample is binned according to fixed steps in comoving volume (a standard ΛCDM cosmology with $\Omega_m = 0.3$ and $h = 0.7$ is used throughout). The complete sample of 910 galaxies from Ferreras et al. (2009) is shown in figure 1. Solid (open) circles represent early-type galaxies whose colours are compatible with an older (younger) stellar population. This simple age criterion is based on a comparison of the observed optical and NIR colours with the predictions from a set of templates with exponentially decaying star formation histories, all beginning at redshift $\mathrm{z_F} = 3$, with solar metallicity. The "old" population is compatible with formation timescales $\tau \lesssim 1$ Gyr (see Ferreras et al. 2009, for details). The black dots in the figure correspond to the sample of 457 galaxies used in this paper.

We further subdivide this sample into three mass bins, starting at $\log(\mathrm{M}_s/\mathrm{M}_{\odot}) = 10.5$ with a width $\Delta \log(\mathrm{M}_s/\mathrm{M}_{\odot}) = 0.5$ dex. For comparison, the characteristic stellar mass from the mass function of the GOODS-MUSIC sample is shown as a dashed line (Fontana et al. 2006), although we warn that the GOODS-MUSIC masses are calculated using a Salpeter (1955) IMF, which will give a systematic 0.25 dex overestimate in $\log\mathrm{M}_s$ with respect to our choice of IMF. Our sample is safely away from the limit imposed by the cut in apparent magnitude ($i_{AB} \leqslant 24$). The curved solid lines give that limit for two extreme star formation histories, corresponding to the "old" and "young" populations as defined above. Notice that within our sample of massive early-type galaxies there are NO galaxies whose colours are compatible with young stellar populations (i.e. open circles).

3 THE EVOLUTION OF MASSIVE GALAXIES

The redshift evolution of the comoving number density is shown in figure 2 (black dots). The (1σ) error bars include both Poisson noise as well as the effect of a 0.3 dex uncertainty in the stellar mass estimates. These uncertainties are computed using a Monte Carlo run of 10,000 realizations. The figure includes data from GOODS-MUSIC (Fontana et al. 2006), COMBO17 (Bell et al. 2004) and Pal/DEEP2 (Conselice et al. 2007). At z=0 we show an estimate from the segregated 2dFGRS luminosity function (Croton et al. 2005). We take their Schechter fits for early-type galaxies within an environment with a mean density defined by a contrast – measured inside radius $8h^{-1}$ Mpc – in the range $\delta_8 = -0.43 \cdots +0.32$ (black open circles). In order to illustrate possible systematic effects in 2dFGRS, we also include the result for their full volume sample as grey open circles. The 2dFGRS data are originally given as luminosity functions in the rest-frame b_J. We took a range of stellar populations typical of early-type galaxies in order to translate those luminosities into stellar masses. The error bars shown for the 2dFGRS data represent the uncertainty caused by this translation from light into mass over a wide range of stellar populations (with typical M/L(b_J) in the range $7 \cdots 12\ \mathrm{M}_{\odot}/\ \mathrm{L}_{\odot}$). The black solid lines show semi-analytic model (SAM) predictions from Khochfar & Silk (2006a). Their SAM follows the merging history of dark matter halos generated by the Extended Press-Schechter formalism down to a mass resolution of $M_{\rm min} = 5 \times 10^9\ \mathrm{M}_{\odot}$, and follows the baryonic physics within these halos using recipes laid out in Khochfar & Burkert (2005, and references therein). The grey dashed lines are the predictions from the Millennium simulation De Lucia et al. (e.g. 2006). This model is extracted from their web-based database[1], and is not segregated with respect to galaxy morphology. This explains the excess number density in the low-mass bin (bottom panel). In the two higher mass bins most of the galaxies have an early-type morphology. The predictions of the Millennium simulation are in agreement with the middle bin – i.e. masses between 10^{11} and $3 \cdot 10^{11}\mathrm{M}_{\odot}$. However, for the most massive bin, the sharp decrease in density with redshift of the models is in remarkable disagreement with the observations. In contrast, Khochfar & Silk (2006a) predict a nearly constant density at the highest mass bin out to z$<$1.

The main reason for this discrepancy is that AGN feedback in the Millennium simulation prohibits the growth of massive galaxies by gas cooling and subsequent star formation in order to reproduce the right colour-bimodality and the luminosity function at z=0. As shown in Khochfar & Silk (2008) the existence of a characteristic mass scale for the shut-off of star formation will lead to dry merging being the main mechanism for the growth of massive galaxies. In that respect the evolution of the number density of massive galaxies in the Millennium simulation is mainly driven by mergers. The difference between that model and Khochfar & Silk (2006a) is probably due to the different merger rates in their models. The Millennium simulation predicts a lower major merger rate compared to Khochfar & Silk (2006a) almost by a factor 10 (Hopkins et al., in preparation).

Figure 3 shows the redshift evolution of the half-light radius. Our methodology follows a non-parametric approach avoiding the degeneracies intrinsic to profile fitting. Nevertheless, we compared our size estimates with those using a parametric approach like GALFIT (Häussler et al. 2007) and there is good agreement (see §2). Our data (black dots) are compared with Trujillo et al. (2007, grey triangles) and with a z$\sim$0 measurement from the SDSS (Shen et al. 2003, taking their early-type sample). The error bars give the RMS scatter of the size distribution within each mass and redshift bin. The lines correspond to the models of Khochfar & Silk (2006b). These models associate size evolution to the amount of dissipation encountered during major mergers along the merging history of an early-type galaxy. The points at high redshift (z$>$1.2) correspond to *individual* measurements from the literature (see caption for details). In all the comparisons shown in this paper with work from the literature, we have checked that the initial mass functions used are similar, so that stellar masses are compared consistently. All results quoted either use a Chabrier (2003) IMF or functions very close to it in terms of the total mass expected per

[1] `http://www.mpa-garching.mpg.de/millennium`

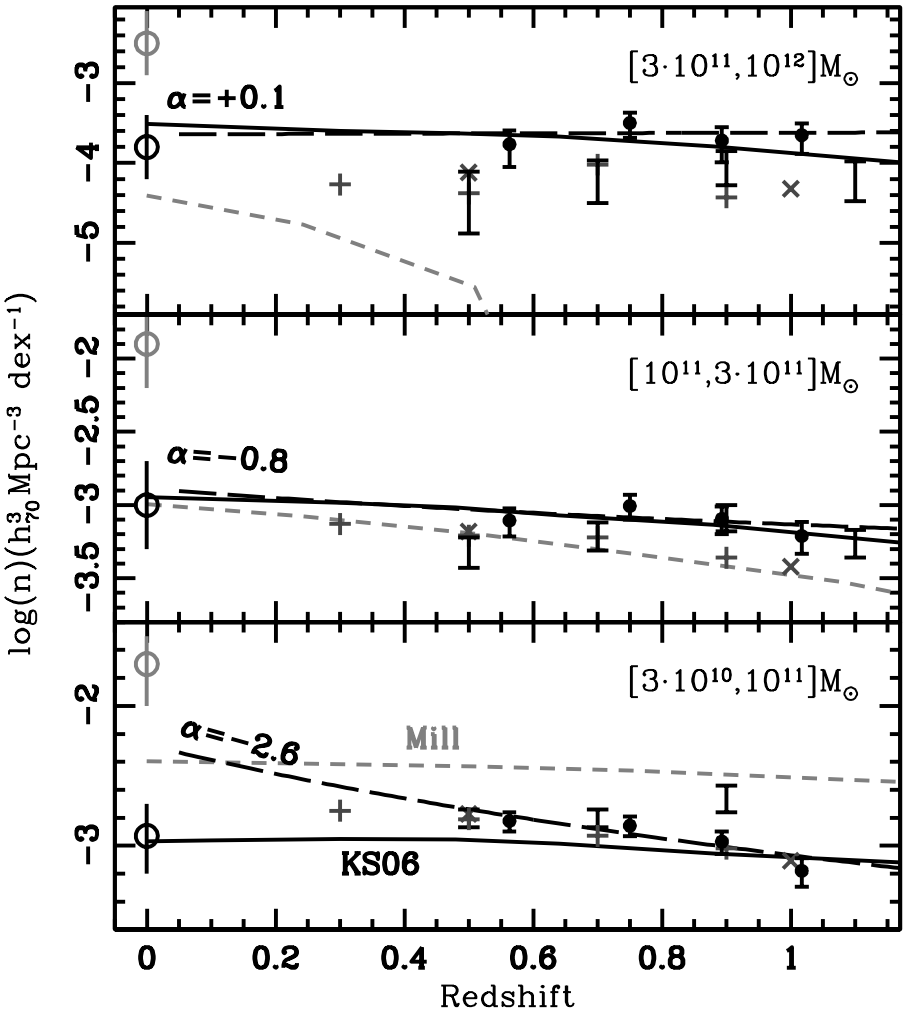

Figure 2. Evolution of the comoving number density of massive early-type galaxies. Our sample (filled dots) is shown for the three mass bins as labelled in the three panels. The points and error bars show the average and standard deviation for each redshift bin, adding in quadrature Poisson noise and the uncertainty in the stellar mass estimate. Other points from the literature are included, namely GOODS-MUSIC ($\times$ signs; Fontana et al. 2006), Palomar/DEEP2 (vertical segments; Conselice et al. 2007) and COMBO17 (+ signs; Borch et al. 2006). The points at z=0 are estimates from 2dFGRS restricted to (spectroscopically classified) early-type galaxies (black/grey open circles corresponding to their mean density sample/full volume; Croton et al. 2005). Notice the density of the most massive galaxies (*top*) does not evolve over the whole redshift range, spanning a look-back time of about 8 Gyr. The black solid lines are model predictions from (Khochfar & Silk 2006a), the grey dashed lines are from the Millennium simulation (e.g. De Lucia et al. 2006, ; no morphology segregation) and the black dashed lines are fits to a power law: $n \propto (1+z)^{\alpha}$, with α given in each panel.

luminosity unit, which – for early-type systems – mainly reduces to the shape of the low-mass end of the IMF. Other functions used in the quoted data were Kroupa et al. (1993); Kroupa (2001) or Baldry & Glazebrook (2003). Only for the GOODS-MUSIC data (Fontana et al. 2006) the Salpeter IMF (1955) was used, which will always give a systematic overestimate of ~ 0.25 dex in stellar mass with respect to the previous choices given its (unphysical) extrapolation of the same power law down to the low stellar mass cutoff (see e.g. Bruzual & Charlot 2003). A single-law Salpeter IMF is an unlikely choice for the stellar populations in early-type galaxies as shown by comparisons of photometry with kinematics (Cappellari et al. 2006) or with gravitational lensing (Ferreras et al. 2008).

Similarly to the density evolution, we also apply a simple power law fit only to our data points: $R_e \propto (1+z)^{\beta}$. The solid lines give those best fits, and the power law index is given in each panel. Taking into account all data points betweeen z=0 and z$\sim$2.5 one sees a clear trend of decreasing size with redshift for all three mass bins. However our data suggest milder size evolution for the most massive early-type galaxies between z=1.2 and z=0.4, corresponding to a 4 Gyr interval of cosmic time.

The depth and high spatial resolution of the ACS images also allow us to probe in detail the *intrinsic* colour distribution of the galaxies (i.e. the colour distribution within each galaxy). We follow the approach described in Ferreras et al. (2005) which, in a nutshell, registers the images in the two bands considered for a given

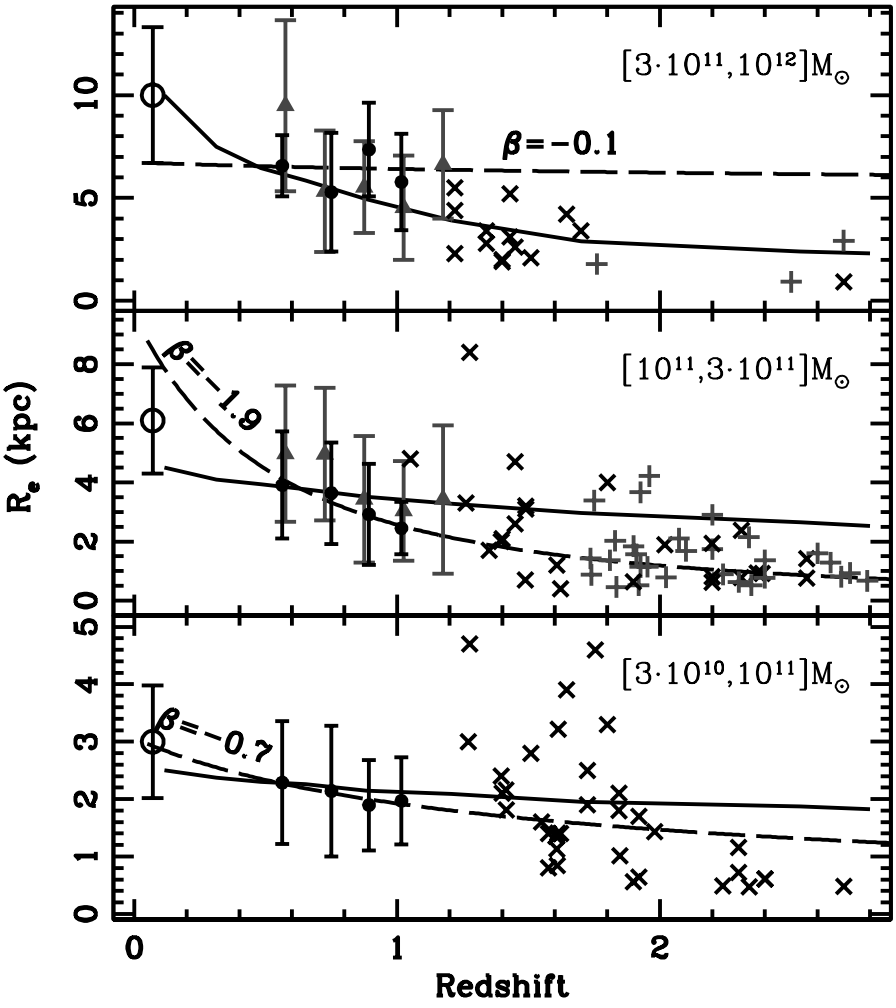

Figure 3. Redshift evolution of the half-light radius. Our sample is shown as filled black circles. The data from Trujillo et al. (2007) is shown as grey triangles and the z∼0.1 sizes of SDSS early-type galaxies are shown as open circles (Shen et al. 2003). At higher redshifts we include *individual* measurements from Buitrago et al. (2008, grey '+' signs) and from other recent work in the literature ('x' signs: Zirm et al. 2007; Toft et al. 2007; van Dokkum et al. 2008; Cimatti et al. 2008). The solid lines are the predictions from Khochfar & Silk (2006b), and the dashed lines are fits to a power law: $R_e \propto (1+z)^{\beta}$, with the power law exponent given in each panel.

colour, degrades them by the Point Spread Function of the other passband, and perfoms an optimal Voronoi tessellation in order to achieve a S/N per bin around 10 while preserving spatial resolution. The final binned data is used to fit a linear relation between colour and $\log(R/R_e)$ from which we determine the slope and the scatter about the best fit (using a biweight estimator). Figure 4 shows the observer-frame V−i colour gradient (*bottom*) and scatter (*top*) as a function of stellar mass (*left*) and half-light radius (*right*). The black dots correspond to binned data in stellar mass, showing the average and RMS value within each bin. Notice the significant trend with increasing stellar mass towards redder cores (i.e. more negative colour gradients) and small scatter. The colour gradient is in most cases nearly flat, and only for the lowest mass bin do we find significantly large gradients. For comparison, we also show as small grey dots a continuation of the original sample from Ferreras et al. (2009) towards lower stellar masses. Blue cores (positive colour gradients) dominate in spheroidal galaxies below $10^{10}\mathrm{M}_{\odot}$. The homogeneous intrinsic colour distribution thereby suggests no significant star formation and a fast rearranging process of the stellar populations if mergers take place during the observed redshift range. Notice this sample only targets objects visually classified as early-type galaxies. The early phases of major merging are therefore excluded from our sample. Nevertheless, the number density at the massive end (upper panel of figure 2) does not change significantly between z=0 and z∼1, already suggesting that major merger events must be rare over those redshifts.

4 DISCUSSION AND CONCLUSIONS

Using a volume-limited sample of massive spheroidal galaxies from the v2.0 ACS/HST images of the GOODS North and South

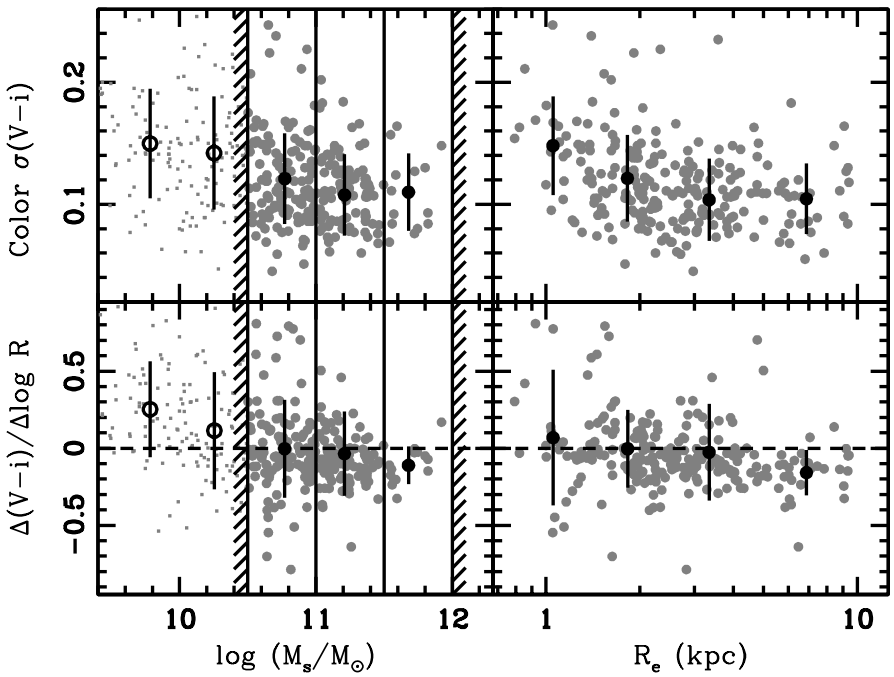

Figure 4. The radial colour gradient ($\Delta(\mathrm{V}-\mathrm{i})/\Delta \log R$; bottom) and RMS scatter (top) is shown as a function of stellar mass (*left*) and projected physical half-light radius (*right*). Negative (positive) gradients imply galaxies with red (blue) cores. The three mass bins used in this paper are illustrated by the vertical lines and the hatched regions in the left-hand panels. The average and RMS values within each bin is shown by the black dots and error bars. Hollow dots in the left-hand panels give the values for two bins outside of our adopted mass range, for comparison. The figure shows the trend of a reduced scatter – concentrating the distribution towards a slightly red core – as mass increases.

fields we have consistently estimated the number density, size and intrinsic colour distribution over the redshift range $0.4<z<1.2$. In combination with other samples we find a significant difference in the redshift evolution according to stellar mass, in agreement with recent work based on other samples or different selection criteria (see e.g. Bundy et al. 2005; McIntosh et al. 2005; Franceschini et al. 2006; Fontana et al. 2006; Borch et al. 2006; Brown et al. 2007; Trujillo et al. 2007; van Dokkum et al. 2008). The most massive galaxies – which impose the most stringent constraints on models of galaxy formation – keep a constant comoving number density between $z\sim1$ and 0 (i.e. over half of the current age of the Universe) but present a significant size evolution, roughly a factor 2 increase between z=1 and 0. Note, however that within our sample, there is no significant size evolution over the redshift range $z=0.4\cdots1.2$. It is by extending the analysis to higher redshifts that the size evolution shows up at the most massive bin (e.g. van Dokkum et al. 2008; Buitrago et al. 2008). When velocity dispersion is added to the analysis, a significant difference is found in the σ-R_e distribution between z=0 and z=1, suggesting an important change in the dynamics of these galaxies (van der Wel et al. 2008).

Some of the semianalytic models of massive galaxy evolution (Khochfar & Silk 2006a,b) are in good agreement with these observations. These models follow the standard paradigm of early-type galaxy growth through major mergers, with the ansatz that size evolution is related to the amount of dissipation during major mergers. The decreasing evolution in the comoving number density at high masses is explained within the models by a balance between the 'sink' (loss due to mergers of massive galaxies generating more massive galaxies) and 'source' terms (gain from mergers at lower mass) over the redshifts considered. One could argue that the sink terms would generate a population of extremely massive galaxies (above a few $10^{12}\mathrm{M}_\odot$), possibly the central galaxies within massive groups or clusters. However, this population – with predicted comoving number densities below $10^{-6}\mathrm{Mpc}^{-3}$ – are very hard to study with current surveys. Furthermore, environment effects in these systems will complicate the analysis of size evolution (e.g. Khochfar & Ostriker 2008).

It is important to note that the lack of evolution in the number density relates to the bright end of the luminosity function. Faber et al. (2007) found a significant change in the number density of *red* galaxies with redshift. However, they also emphasize that this change does not refer to the most luminous galaxies. If we include all mass bins in our sample, we do find a significant decrease in the number density with redshift, as the lower mass bins – which contribute the most in numbers – do have a rather steep decrease in density (see figure 2). This difference suggests that the (various) mechanisms playing a role in the transition from blue cloud to red sequence must be strongly dependent on the stellar mass of the galaxies involved.

In a more speculative fashion, our data are also suggestive of weak or even *no evolution* in the number density of the most massive early-type galaxies over a redshift range $0.4<z<1.2$. This would imply a negligible role of major mergers at the most massive end for $z>0.4$, thereby pushing this stage of galaxy formation towards lower redshifts (Khochfar & Silk 2008). Another speculative scenario for the evolution of massive spheroidal galaxies would involve negligible major mergers at these redshifts and a significant

amount of minor mergers which will 'puff up' the galaxy. Minor mergers are considered the cause of recent star formation observed in NUV studies of early-type galaxies (Kaviraj et al. 2007). Larger surveys of Luminous Red Galaxies are needed to confirm or disprove this important issue.

REFERENCES

Baldry, I. K. & Glazebrook, K., 2003, ApJ, 593, 258
Bell, E. F. et al. 2004, ApJ, 608, 752
Bershady, M. A., Jangren, A. & Conselice, C. J., 2000, AJ, 119, 2645
Borch, A., et al. , 2006, A& A, 453, 869
Bower, R. G, Benson, A. J., Malbon, R., Helly, J. C., Frenk, C. S., Baugh, C. M., Cole, S. & Lacey, C. G. 2006, MNRAS, 370, 645
Brown, M. J. I., Dey, A., Jannuzi, B. T., Brand, K., Benson, A. J., Brodwin, M., Croton, D. J. & Eisenhardt, P. R., 2007, ApJ, 654, 858
Bruzual, G. & Charlot, S., 2003, MNRAS, 344, 1000
Buitrago, F., Trujillo, I., Conselice, C. J., Bouwens, R. J., Dickinson, M. & Yan, H., 2008, arXiv:0807.4141
Bundy, K., Ellis, R. S. & Conselice, C. J., 2005, ApJ, 625, 621
Cappellari, M., et al. , 2006, MNRAS, 366, 1126
Chabrier, G., 2003, PASP, 115, 763
Cimatti, A., et al. , 2008, A& A, 482, 21
Conselice, C. J., et al. , 2007, MNRAS, 381, 962
Croton, D. J., et al. 2005, MNRAS, 356, 1155
Damjanov, I., et al. 2008, arXiv:0807:1744
De Lucia, G., Springel, V., White, S. D. M., Croton, D. & Kauffmann, G. 2006, MNRAS, 366, 499
Faber, S. M., et al. , 2007, ApJ, 665, 265
Ferreras, I., Lisker, T., Carollo, C. M., Lilly, S. J. & Mobasher, B. 2005, ApJ, 635, 243
Ferreras, I., Saha, P. & Burles, S. 2008, MNRAS, 383, 857
Ferreras, I., Lisker, T., Pasquali, A. & Kaviraj, S. 2009, MNRAS submitted, arXiv:0901.2123
Fontana, A., et al. 2006, A& A, 459, 745
Franceschini, A., et al. , 2006, A& A, 453, 397
Giavalisco, M., et al. , 2004, ApJ, 600, L93
Graham, A. W., Driver, S. P., Petrosian, V., Conselice, C. J., Bershady, M. A., Crawford, S. M. & Goto, T. 2005, AJ, 130, 1535
Grazian, A. et al. , 2006, A& A, 449, 951.
Häussler, B. et al. , 2007, ApJS, 172, 615
Kaviraj, S., Devriendt, J. E. G., Ferreras, I., Yi, S. K. & Silk, J. 2006, arXiv:astro-ph/0602347
Kaviraj, S., Peirani, S., Khochfar, S., Silk, J. & Kay, S., 2007, MNRAS, in press, arXiv:0711.1493
Khochfar, S. & Burkert, A. 2005, MNRAS, 359, 1379
Khochfar, S. & Ostriker, J. P. 2008, ApJ, 680, 54
Khochfar, S. & Silk, J. 2006a, MNRAS, 370, 902
Khochfar, S. & Silk, J. 2006b, ApJ, 648, L21
Khochfar, S. & Silk, J. 2008, arXiv:0809.1734
Kroupa, P., Tout, C. A. & Gilmore, G., 1993, MNRAS, 262, 545
Kroupa, P., 2001, MNRAS, 322, 231
McIntosh, D., et al. , 2005, ApJ, 632, 191
Renzini, A. 2006, ARA& A, 44, 141
Salpeter, E. E., 1955, ApJ, 121, 161
Shen, S., Mo, H. J., White, S. D. M., Blanton, M. R., Kauffmann, G., Voges, W., Brinkmann, J. & Csabai, I. 2003, MNRAS, 343, 978
Toft, S., 2007, ApJ, 671, 285
Trujillo, I., Conselice, C. J., Bundy, K., Cooper, M. C., Eisenhardt, P., & Ellis, R. S. 2007, MNRAS, 382, 109
van der Wel, A., Holden, B. P., Zirm, A. W., Franx, M., Rettura, A., Illingworth, G. D. & Ford, H. C., 2008, arXiv:0808.0077
van Dokkum, P. G., et al. 2008, ApJ, 677, L5
Zirm, A. W., et al. 2007, ApJ, 656, 66